# Estimating maximum installable power for groundwater extraction across Africa

Guillaume Zuffinetti[a,b], Simon Meunier[a,b,*], Donald John MacAllister[c], Peter K. Kitanidis[d], Alan M. Macdonald[c]

[a] Université Paris-Saclay, CentraleSupélec, CNRS, GeePs, 91192 Gif-sur-Yvette, France

[b] Sorbonne Université, CNRS, GeePs, 75252 Paris, France

[c] British Geological Survey, The Lyell Centre, Research Avenue South, Edinburgh EH14 4AS, Scotland, United Kingdom

[d] Department of Civil and Environmental Engineering, Stanford University, Stanford, United States

[*]Corresponding author: Simon Meunier (simon.meunier@centralesupelec.fr)

**Abstract:** Groundwater development is the most likely way to meet growing global water demand but needs careful management. To help inform the sustainable development of groundwater resources, we develop a novel indicator based on the maximum installable power for water pumping systems and apply it to Africa. Here, we first map a maximum annual pumpable volume across Africa with a 0.2-degree resolution, considering available aquifer recharge and storage. Using a water pumping system model, the maximum power that can be installed per km$^2$ without exceeding the maximum annual pumpable volume is conservatively computed. Constrained by recharge (considering 25% of the annual recharge), the maximum installable power ranges between 0 and 5000 W/km$^2$ across Africa with regions such as the Congo Basin (~198 W/km$^2$), and western Africa between the Ivory Coast and Nigeria (~136 W/km$^2$) identified as having high potential for sustainable pumping system development. Constrained by storage (considering 0.1% of storage), it ranges between 0 and 6800 W/km$^2$ highlighting the ability to deplete storage for pumping system development in the large aquifers northern Sahara (~3800 W/km$^2$). These findings provide a novel and adaptable way to examine water security, which can assist institutions in targeting investments to meet water demand sustainably.

# Main

Water consumption for human uses is projected to increase in Africa[1], notably due to the high population growth which is expected to occur in this continent by 2050[2]. Water demand will be driven by increases in domestic water consumption, industry[3], and irrigation for food production[4] especially in Sub-Saharan Africa where only 5% of cultivable land is currently irrigated[5]. To respond to this future water demand, groundwater represents the main store of freshwater in Africa[6]. Furthermore, contrary to surface water, groundwater often does not require treatment[7] and is also less vulnerable to weather conditions, acting therefore as a natural buffer against climate unpredictability[8–11]. However, groundwater over abstraction can have severe consequences, such as reducing baseflow to rivers[12], drying out shallow wells[13], increasing pollution[14,15] or even sea level rise[16,17].

Hence, further development of groundwater must be sustainable. The Sustainable Development Goal 12 (Ensure sustainable consumption and production patterns) calls for a better management and use of natural resources[18]. Quantitative indicators to measure sustainability for groundwater are thus needed. Decline of groundwater level, measured locally in wells[19,20] or computed at the basin scale by gravity measurements[21], is an example of an indicator used to quantify groundwater over extraction. However, this type of indicator shows where problems have already arisen and therefore does not provide information to help prevent it. Another way to measure sustainability for groundwater resources is to compare the groundwater demand with the groundwater availability[22–25]. Nevertheless, references [22] and [23] did not map their results and only considered near-surface groundwater. Reference [24] mapped an estimation of the unsustainable use of groundwater thanks to the water balance between the aquifer recharge and the abstraction and reference [25] also considered the necessary groundwater contribution to environmental streamflow. However, both used simulated data from 1958 to 2000 for the recharge with a 0.5-degree resolution, while more recent observational data have been established[26]. Finally, a simple indicator is provided by the Sustainable Development Goal 6 (Ensure availability and sustainable management of water and sanitation for all) which calls for the water withdrawal to be lower than 25% of the annual renewability [27]. Nonetheless, this indicator, and to our best knowledge, every existing indicator to measure sustainability for groundwater, are referring to a maximum pumpable groundwater volume not to exceed[12,19–25] which are data hard to measure and control by governments, local authorities, etc[28–30]. An indicator to measure sustainability for the groundwater resources based on the installed power of water pumping systems (WPSs) would be easier to control as shown by agricultural censuses[31,32], more specifically for photovoltaic WPSs[33,34]. In addition, an indicator based on the installed power of WPSs would represent an indicator more convertible into an economic value for a project manager than a maximum pumpable volume thanks to economic models of photovoltaic WPSs[35,36] or diesel WPSs[37] that link the power of the system to its economic value.

Consequently, the novel contribution of this work is the development of a new indicator to measure sustainability for groundwater based on the maximum power that can be installed for WPSs over a unit area. Thanks to this type of indicator, any government, local authority, project owner, etc. will know that if the sum of the installed power of all the WPSs in a given area overshoots a given value, there is a risk of over extraction. In this article, we apply this indicator to the African continent. The first objective is to map a maximum annual volume that can be pumped at each location across Africa according to criteria of sustainability or practicality. This maximum annual pumpable volume at a location is estimated through high-resolution and up-to-date groundwater recharge and storage data at the continental scale with a 0.2-degree resolution (see 'Estimation of the maximum annual pumpable volume' in the Methods Section). In the whole article, this maximum annual pumpable volume is normalized by unit of surface (i.e., the results are shown with dimensions of length/time, such as $m^3/m^2$/year). The second objective is to map the maximum installable power (MIP) for WPSs at each location across Africa, defined as the sum of the power of every WPS that can be installed in a 1 $km^2$ area at this location not to overshoot the maximum annual pumpable volume. To estimate the MIP, we develop a WPS model, based on a generic WPS architecture (see Box 1), which estimates, for each location of Africa with a 0.2-degree resolution, the volume annually pumpable by a WPS of installed power $P_0$. In this article, $P_0$ is equal to 100 W (see 'Estimation of the maximum installable power' in the Methods Section). To do so, the model dynamically simulates the evolution of the pumped flow rate in the borehole with a 2-min time step, whether the aquifer is confined or unconfined (see 'Estimation of the maximum installable power' in the Methods Section). We also provide a method to estimate the maximum remaining power that can be installed for new WPSs by considering the current groundwater withdrawal.

In the core of the article, we only consider immersed water pumping systems (WPSs) (motor-pump or hand-pump). A scenario that considers surface water pumping systems is also provided in the Supplemental note 1. The pump can be supplied by different energy sources: photovoltaic modules, diesel generator, wind turbines, manpower or can be connected to the main electricity grid. The considered WPS architecture is presented in Figure 1. In the case of a motor-pump, control equipment is installed between the energy source and the motor-pump and/or integrated to the motor-pump set in the borehole[38,39]. This equipment allows the motor-pump to stop and prevents it from running dry[35]. It also allows the motor-pump to operate at its best operating points[38].

Figure 1 also shows the layout of a borehole. $r_b$ is the borehole radius and $H_{b,s}$ is the static water level, which corresponds to the water depth in the borehole when there is no pumping. $H_{st}$ is the saturated thickness of the aquifer, $H_{b,b}$ is the borehole depth and $H_{pu}$ is the pump depth. When pumping starts, a drawdown $H_{b,d}$ is formed in the borehole (see Figure 1). The higher the pumped flow rate, the higher the drawdown $H_{b,d}$, and therefore the deeper the water in the borehole $H_b$. If $H_b$ reaches the position of the pump $H_{pu}$, the pump remains shut down during a period $\Delta t_{shut}$ (see Supplementary Figure 3) after which it attempts to restart. It is done automatically in the case of a motor-pump and by hand in the case of a hand-pump[35,40]. All the dimensions in Figure 1 are defined as positive.

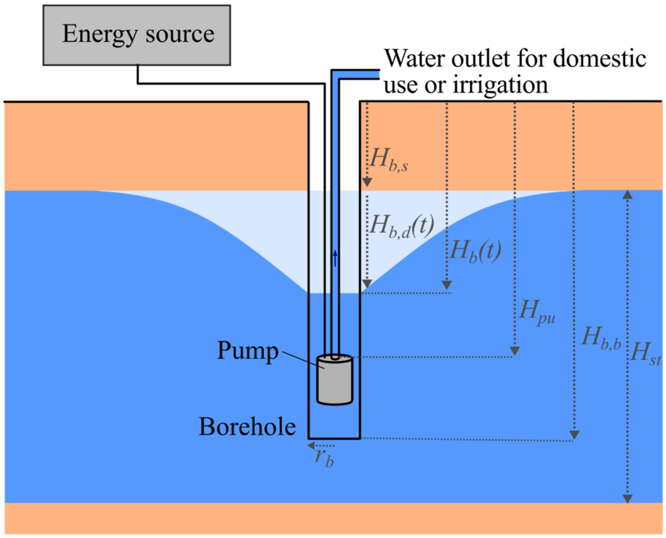


*Figure 1 – Considered generic water pumping system architecture*

*Box 1 - Water pumping system description, architecture and operation*

To fulfil these objectives, input location-dependent data and WPS design parameters are required. They are listed respectively in Table 1 and in Table 2. To ensure the conservativity of our results, the choice of both input location-dependent data and design parameters values relies on conservative assumptions (see 'Conservative assumptions and choice of the design parameters' in the Methods Section). In Table 2, we present the design parameters values chosen for this article. In Figure 2, we plot the values for the groundwater recharge $R$, the aquifer transmissivity $T$, the saturated thickness $H_{st}$, the static water level $H_{b,s}$, the groundwater storage $S$ and the water withdrawal for domestic use in 2010 that we use for the rest of the article.

| Data | Symbol | Description | Spatial resolution | Temporal resolution and coverage | Year of release | Provider |
|---|---|---|---|---|---|---|
| Aquifer recharge (m/year) | $R$ | Groundwater recharge refers to the hydrological process by which water flows from surface water sources and infiltrates into the groundwater system | 0.2° | One value for each location | 2021 | British Geological Survey[6,26,40,41] |
| Aquifer transmissivity ($m^2/s$) | $T$ | Rate at which groundwater flows horizontally through an aquifer | | One range of variation for each location | 2012 | |
| Aquifer saturated thickness (m) | $H_{st}$ | Vertical thickness of the hydrogeologically designated aquifer layer where the pores are filled with water | | | | |
| Static water level (m) | $H_{b,s}$ | Water level in the borehole when no pumping is occurring | | | | |
| Groundwater storage (m) | $S$ | Groundwater storage in the aquifer defined as a water depth | 0.05° | | | |
| Water withdrawal (mm/month) | – | Water withdrawal for domestic use, mining, generating electricity, manufacturing, livestock and irrigation | 0.5° | Data available for each month between 1970 and 2010 | 2018 | Huang et al.[42] |

*Table 1 - Input location-dependent data*

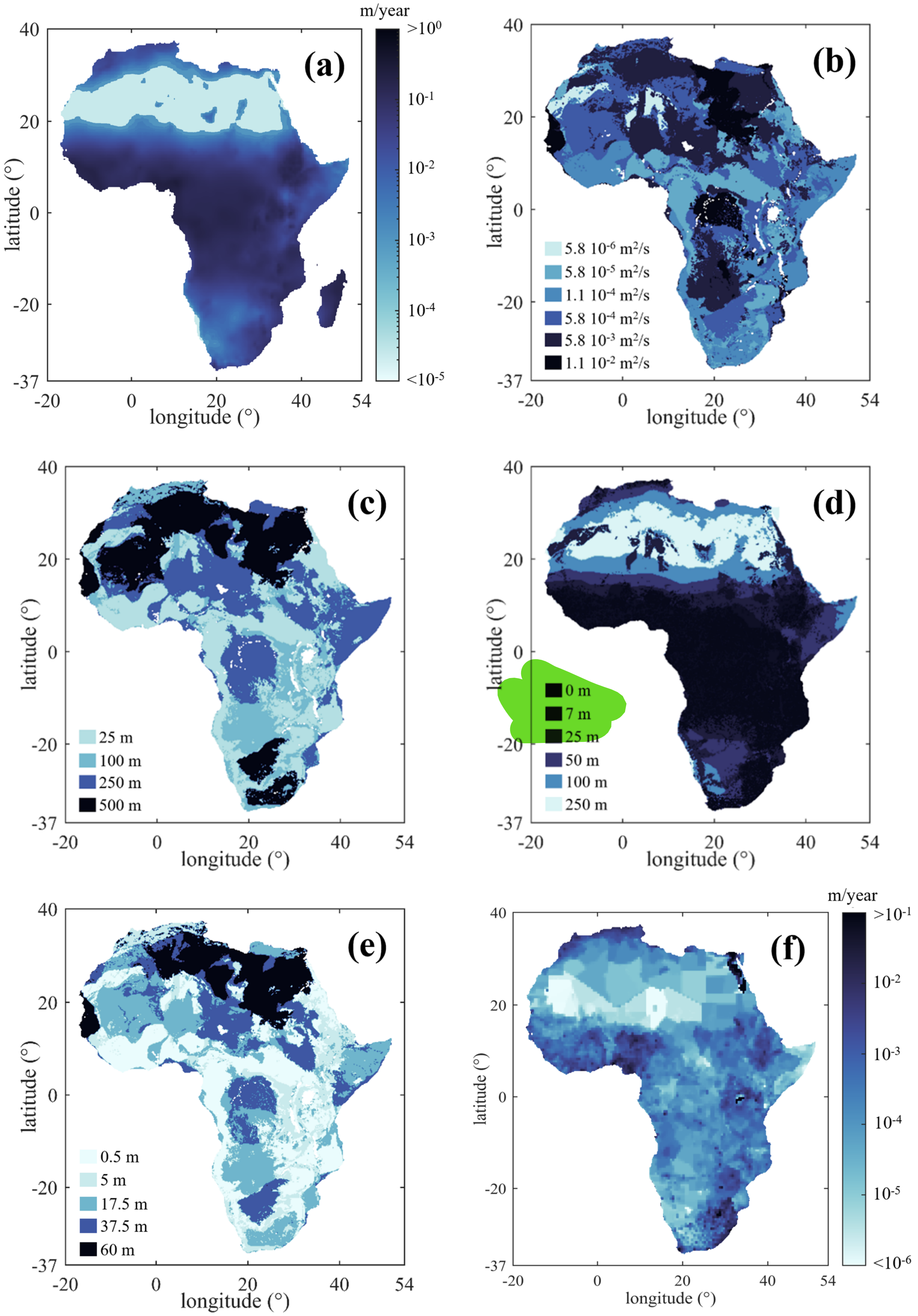


*Figure 2 - Representation of selected input location-dependent data: (a) groundwater recharge R, (b) aquifer transmissivity T, (c) aquifer saturated thickness $H_{st}$, (d) static water level $H_{b,s}$, (e) groundwater storage S and (f) water withdrawal for domestic use in 2010*

| Design parameter | Symbol | Value considered |
| --- | --- | --- |
| Input power of the pump (W) | $P_0$ | 100 W[40] |
| Pump efficiency (-) | $\eta_{pu}$ | 0.7[43–46] |
| Minimum shutdown time of the pump before attempting to restart (min) | $\Delta t_{shut}$ | 30 min[35] |
| Borehole radius (m) | $r_b$ | 0.3 m[40] |
| Borehole losses coefficient ($s^2/m^5$) | $\beta$ | $5{\cdot}10^4$ $s^2/m^5$ [47,48] |
| Pump depth (m) | $H_{pu}$ | In order to minimize the risk of frequent pump stoppages due to the drawdown reaching the pump, while leaving a margin to prevent sand at the bottom of the borehole from entering the pump, the pump is positioned 10 m above the borehole bottom[49]. |
| Borehole depth (m) | $H_{b,b}$ | If the saturated thickness is equal to 25 m, the borehole depth is set to $H_{b,s} + H_{st} + 10$ and the pump is thus at the bottom of the saturated thickness in this case[40].<br>For saturated thicknesses larger or equal to 100 m, the borehole depth is set to $H_{b,s}$ + 60 m[40]. This enables significant intersection of the saturated thickness while avoiding excessive drilling costs[50]. |
| Linear pipes losses coefficient ($s^2/m^6$) | $\gamma$ | 4.7 $s^2/m^6$ [36] obtained by considering a pipe of diameter $D_p$ of 0.15 m[51] and of roughness $\epsilon$ of 0[52] (see reference [40]). |
| Junction losses coefficient ($s^2/m^5$) | $K$ | 209 $s^2/m^5$ [36] which corresponds to one 90° regular threaded elbow for a pipe of diameter $D_p$ of 0.15 m[40]. |
| Pipes length (m) | $L_p$ | $L_p$ is taken equal to the pump depth. |

*Table 2 - Considered values of the design parameters*

# Results

In the following, every result is shown either by considering that the percentage of the annual recharge that we accept to pump is $\alpha_R$ = 25%[27] and the percentage of the groundwater storage that we accept to pump each year is $\alpha_S$ = 0 %/year or by considering that $\alpha_R = 0\%$ and $\alpha_S$ = 0.1 %/year. These values are debatable[53] and subject to political decisions, however the first falls from the sustainable development goals, and the second is a pragmatic indicator for mining groundwater storage used by others[54]. We provide an HTML link in the Supplementary information accessible through a downloadable .zip file allowing to show the same results by considering other values of $\alpha_R$ and $\alpha_S$.

**Estimation of the maximum annual pumpable volume.** Figure 3 shows estimates of the maximum annual pumpable volume $V_{max}$ ($m^3/m^2$/year) shown as a depth of water, when $\alpha_R$ = 25% and $\alpha_S$ = 0 %/year (Figure 3a) and when $\alpha_R$ = 0% and $\alpha_S$ = 0.1 %/year (Figure 3b). The mean value of the maximum annual pumpable volume $V_{max}$ across Africa considering Figure 3a is ~$10^{-2}$ $m^3/m^2$/year while the one considering Figure 3b is ~$2{\cdot}10^{-2}$ $m^3/m^2$/year. Both Figures highlight the spatial heterogeneity of the resource. We notably see on Figure 3a that $V_{max}$ is lower in the Sahara than in western sub-Saharan Africa. This is due to the higher recharge in western sub-Saharan Africa than in the Sahara (see Figure 2a). On the opposite, we see on Figure 3b that $V_{max}$ is lower in western sub-Saharan Africa than in the Sahara. This is due to the higher storage in the Sahara than in western sub-Saharan Africa (see Figure 2e).

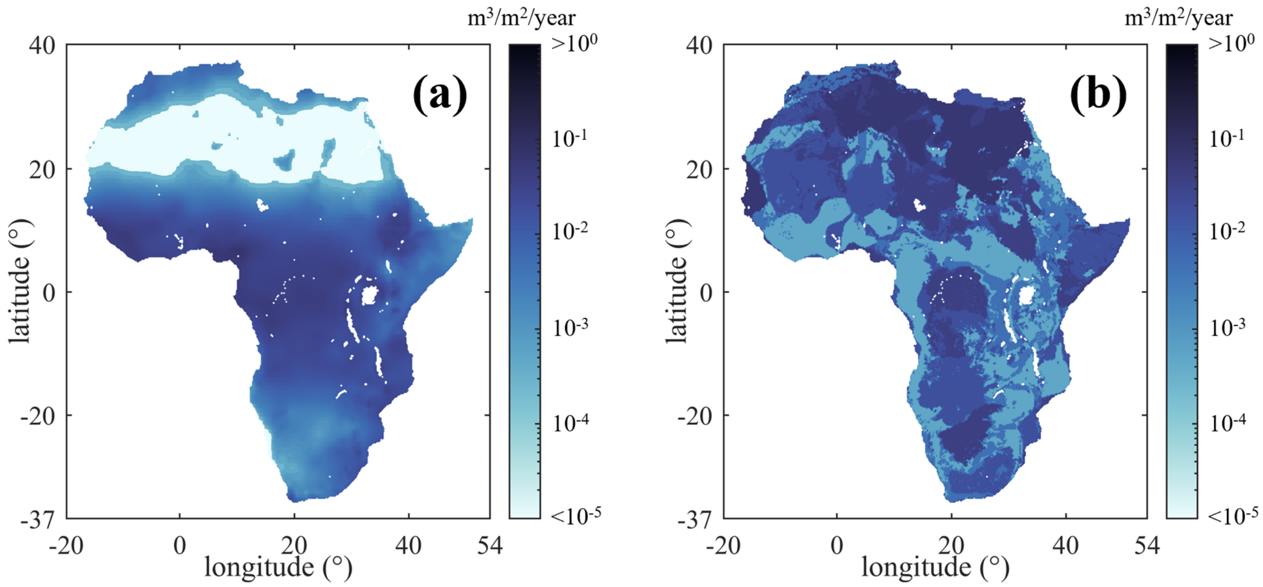


*Figure 3 - Maximum annual pumpable volume $V_{max}$ (m$^3$/m$^2$/year) shown as an equivalent water depth when (a) the percentage of the annual recharge that we accept to pump is $\alpha_R$ = 25% and the percentage of the groundwater storage that we accept to pump each year is $\alpha_S$ = 0 %/year and when (b) $\alpha_R$ = 0% and $\alpha_S$ = 0.1 %/year*

Supplementary Figure 4 shows the total water withdrawal in 2010 and Supplementary Figure 5 shows the same results as Figure 3 for the maximum annual volume that can still be pumped $V'_{max}$, which accounts for the total water withdrawal in 2010 (see 'Estimation of the maximum annual pumpable volume' in the Methods Section). Locations where $V'_{max} < 10^{-5}$ m$^3$/m$^2$/year are locations where groundwater is already over abstracted. 22% of the locations are already over abstracting groundwater when $\alpha_R$ = 25% and $\alpha_S$ = 0 %/year, especially in northern and eastern Africa. 22% of the locations are also over abstracting groundwater when $\alpha_R$ = 0% and $\alpha_S$ = 0.1 %/year but the regions where the groundwater is overexploited are different. The main differences occur in the northern Sahara where the storage is the highest while the recharge is very low and in the western sub-Saharan Africa where the storage is lower and the recharge higher (see Figures 2a and 2e). However, it is important to keep in mind that, as a very conservative assumption, we consider that all the water withdrawal across Africa comes from groundwater resources (see 'Estimation of the maximum annual pumpable volume' in the Methods Section).

**Estimation of the maximum installable power.** Figure 4 shows conservative values for the maximum installable power (MIP) when $\alpha_R$ = 25% and $\alpha_S$ = 0 %/year (Figure 4a) and when $\alpha_R$ = 0% and $\alpha_S$ = 0.1 %/year (Figure 4b). We see on Figure 4a that the MIP is lower in the Sahara than in sub-Saharan Africa where regions like the Congo Basin and the region between the Ivory Coast and Nigeria have a high potential in terms of sustainable water pumping systems development (~198 W/km$^2$ and ~136 W/km$^2$ respectively). This is due to the higher value of $V_{max}$ in sub-Saharan Africa than in the Sahara when $V_{max}$ is a portion of the recharge (see Figure 3a). On the opposite, we see on Figure 4b that the MIP is lower in sub-Saharan Africa than in the Sahara notably with the northern Sahara region which has a significant potential in terms of water pumping systems development (~3800 W/km$^2$). This is due to the higher value of $V_{max}$ in the Sahara than in sub-Saharan Africa when $V_{max}$ is a portion of the storage (see Figure 3b).

The MIP values can be compared to typical pump sizes. As an approximation, we can estimate that the installed power of a hand-pump is ~100 W[55], the typical installed power for a motor-pump for domestic use is ~1000 W[40] and the typical one for a motor-pump for irrigation is ~3000 W[40]. On the one hand, the mean value of the MIP across Africa regarding Figure 4a is ~65 W/km$^2$. It means that the average of the maximum number of systems per 100 km$^2$ area across Africa, only considering the recharge, is ~65 hand-pumps or ~6 motor-pumps for domestic use or ~2 motor-pumps for agricultural use. On the other hand, the mean value of the MIP across Africa regarding Figure 4b is ~1000 W/km$^2$. It means that the average of the maximum number of systems per 100 km$^2$ area, only considering the groundwater storage, is ~1000 hand-pumps or ~100 motor-pumps for domestic use or ~33 motor-pumps for agricultural use. At a specific location, it is also possible to compare the MIP value to installed capacities, when such information is available. For instance, on Figure 4a, the location at 10.6° (lat) & 36.75° (lon), which corresponds to a location in the division of Bure in Ethiopia, has a MIP of ~150 W/km$^2$. This means that in a 100 km$^2$ area at this location, we can install ~150 hand pumps or ~15 motor-pumps for domestic use or ~5 motor-pumps for agricultural use. As a comparison, thanks to the rural decision support tool from the Water Point Data Exchange[56], we count ~38 submersible WPSs including 1 hand-pumps in the ~800 km$^2$ Bure division, which corresponds to an average of ~0 hand pumps and ~5 submersible motor-pumps per 100 km$^2$ area. When analysing these results, it is important to keep in mind that our results are conservative. In addition, these results depend on the chosen values for $\alpha_R$ and $\alpha_S$. Finally, our results are large scale analyses and local studies of the water resources and hydrogeology would be required when planning system installations.

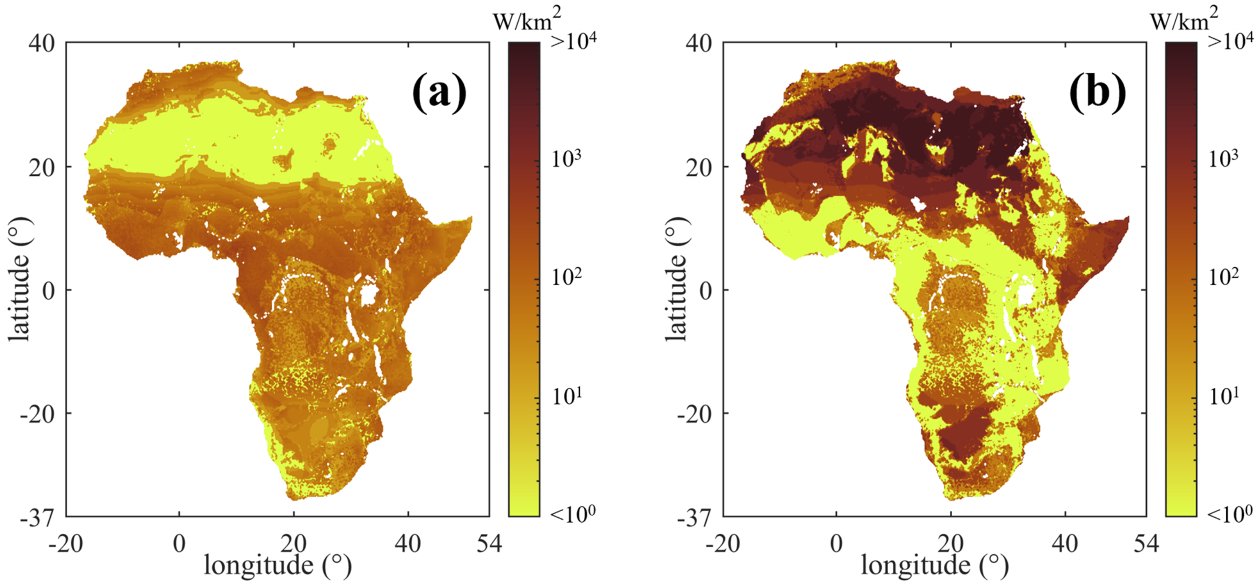


*Figure 4 - Maximum installable power MIP when (a) $\alpha_R$ = 25% and $\alpha_S$ = 0 %/year and when (b) $\alpha_R$ = 0% and $\alpha_S$ = 0.1 %/year*

To estimate the maximum remaining installable power for new WPSs, we substitute $V_{max}$ by $V'_{max}$ while the rest of the method remains the same (see 'Estimation of the maximum installable power' in the Methods Section). Supplementary Figure 6 shows the maximum remaining installable power for new WPSs when $\alpha_R$ = 25% and $\alpha_S$ = 0 %/year (Supplementary Figure 6a) and when $\alpha_R$ = 0% and $\alpha_S$ = 0.1% (Supplementary Figure 6b). A value under $10^{-5}$ W/km$^2$ for the maximum remaining installable power represents regions where water is already over abstracted. On the one hand, the mean value of the maximum remaining installable power for new WPSs across Africa according to Supplementary Figure 6a is ~45 W/km$^2$. On the other hand, the mean value of the maximum remaining installable power for new WPSs across Africa according to Supplementary Figure 6b is ~950 W/km$^2$. Results indicate that, while some regions are over abstracting, other regions like the northern Sahara, the Congo Basin and the region between the Ivory Coast and Nigeria could receive important investments for new WPSs. We also see on Supplementary Figure 6a that the main region where the groundwater resources are already over abstracted, with respect to the recharge, is in the north of Sahara because of the low recharge in this region. Regarding the Supplementary Figure 6b, we see that the main regions that are stressed, with respect to the storage, are on the outlines of sub-Saharan Africa due to the low storage and the high withdrawal in these regions. Nevertheless, these maps should be put in perspective with the conservative assumption made when considering that the total water withdrawal is equal to the total groundwater withdrawal (i.e., all the water is extracted from groundwater). Thus, field studies are very important to obtain a better estimation of the current groundwater withdrawal.

## Discussion

Our results highlight regions with a high potential in terms of installable power for WPSs. However, to develop such systems, it is also important to consider their different operational requirements according to their usage. For instance, to ensure their proper functioning, hand pumps require an aquifer productivity ~0.1 l/s (equivalent to an aquifer transmissivity ~$3.4 \cdot 10^{-5}$ m$^2$/s [57]), small motorized pumps for domestic use require ~5 l/s (equivalent to an aquifer transmissivity ~$4.3 \cdot 10^{-4}$ m$^2$/s [57]) and motorized pumps for irrigation can require an aquifer productivity higher than 20 l/s (equivalent to an aquifer transmissivity ~$5.8 \cdot 10^{-3}$ m$^2$/s [41])[58]. Thus, while hand pumps or small motorized pumps for domestic use have a high deployment potential throughout the continent, the potential for motorized pumps for irrigation is lower (see Figure 2b). As a result, even though the potential in terms of installable power for water pumping systems in relation to the recharge is high in countries like Gabon and Cameroon, this potential could unfortunately only be little used for irrigation due to the low productivity of the aquifers on which these countries rely. On the contrary, highly productive aquifers with also a high potential in terms of installable power for WPSs, such as in Central Africa or Angola, thus appear to have a high potential for the deployment of motorized WPSs for irrigation. To develop irrigated agriculture at a continental scale, more research is needed on water pumping systems for irrigation to reduce this constraint on the aquifer productivity[59].

Moreover, there are also economic constraints to the development of WPSs in regions where the groundwater resources are poorly accessible[60]. Indeed, the deeper the borehole, the more expensive the installation of the WPS[58]. Therefore, even if the potential in terms of installable power for WPSs in relation to storage is high in the Sahara, the high depth to the water table in this region make the access to the resource very expensive. Governments or supranational organizations could then help fund programs to deploy WPSs in such areas to help provide access to improved water for all. Regions with extreme poverty[61] may be prioritized like in Niger[62] or in the horn of Africa[63]. However, the opposite situation, areas where the groundwater resource is easily accessible while the potential in terms of installable power for WPSs is low, can also represent a challenge regarding the overexploitation of the resource (such areas can notably be identified by comparing static water level maps to Figure 4). In particular, alluvial aquifers, which are generally easily accessible from an economic point of view[64], with a low potential in terms of installable power, such as the Congo Delta Coastal Sedimentary Basin aquifer[65], should be closely monitored. As it is a more easily controllable indicator, the MIP can help countries which lack of groundwater-monitoring systems[60]. In addition, due to rapid population growth which leads to an increase of the water need, demands for borehole permits or groundwater abstraction licences are increasing and are becoming hard to control[66]. Consequently, a more easily controllable indicator such as the MIP could support this kind of initiatives and licences on the installed power for WPSs could be envisaged. Such licences could for instance be controlled during agricultural censuses[32].

Finally, it is interesting to compare the results to the population density[67], which is plotted in Figure 5. Comparing this Figure 5 to Figure 4 allows to identify dense regions where it is also possible to largely deploy WPSs without regionally threatening groundwater resources. This is notably the case in parts of the Mediterranean coast and in West Africa. Groundwater resources are already highly exploited in northern Africa[68], but for a country, such as Benin which weakly relies on groundwater[68] there could be more potential for groundwater development[69]. We also see that parts of the continent, such as Congo Basin, the Sahara and southeast Africa have a high potential for the deployment of WPSs by using groundwater storage but a relatively low population density. Some schemes have been developed to reticulate water to neighbouring regions such as the man made river project in Libya[70], however the economic and environmental benefits are challenging. Consequently, our results also reinforce the interest for the sustainable management of transboundary aquifers. Indicators such as the MIP along with other indicators could help inform such processes[71].

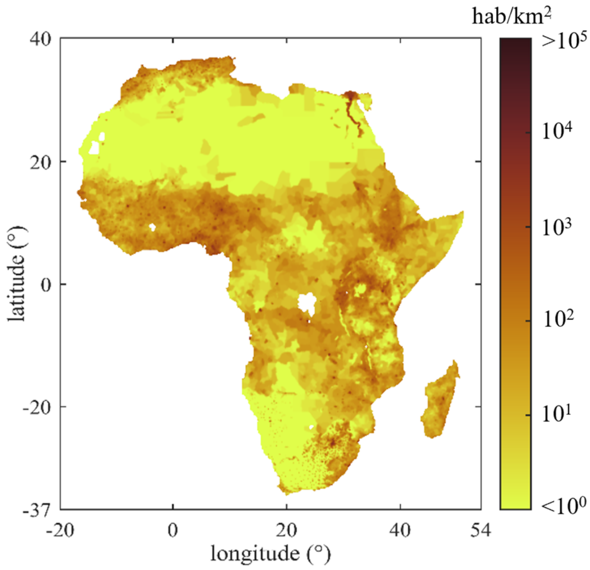


*Figure 5 - Population density[67]*

# Conclusion

We propose a model that uses recent publicly and freely available groundwater and water withdrawal data to provide a novel indicator to measure sustainability for groundwater based on the maximum installable power (MIP) for any location in Africa with a resolution of 0.2°. The model, which accounts for the different components of the water pumping system (WPS), notably simulates dynamically the evolution of the pumped flow rate and of the drawdown with a 2-min time step, whether the aquifer is confined or unconfined. Results indicate a strong spatial variability of the MIP. Results show that, when the groundwater extraction threshold is defined by the recharge, the Congo basin and the region between the Ivory Coast and Nigeria have a high potential for WPSs while. When examining groundwater mining from storage, the aquifers beneath the Sahara are highlighted. When considering the current water withdrawal as a proxy for the current groundwater withdrawal, when the groundwater extraction threshold is equal 25% of the recharge and 0 %/year of the storage, we find that 22% of the locations could already be over abstracting groundwater, especially in northern and eastern Africa. When the groundwater extraction threshold is equal to 0% of the recharge and 0.1 %/year of the storage, 22% of the locations are also stressed but at different locations, with a particular difference in the Sahara because of its large groundwater storage and low recharge.

The limitations of our study are those intrinsic to approaches consisting of evaluating a model to an extensive spatial scale (an entire continent). The groundwater input data have themselves been estimated, concealing the specificity of local resources. Furthermore, since we rely on data available for the entire African continent, our proposed WPS model is less precise compared to a WPS model where we can directly access and measure all site characteristics (e.g., through pumping tests). Consequently, it is important to view the results of this large-scale analysis as an original overview over the continent and as a complement to local analyses that are inherently more accurate.

Despite these limitations, this study gives a conservative estimate of the MIP for WPSs for any location across Africa (without the need to collect additional data). The MIP can be a useful tool for water sector practitioners (e.g. local companies, non-governmental organizations) to use in combination with more traditional indicators. Our results also help to identify regions where local studies on the actual groundwater withdrawal are strongly required before installing new systems in order to ensure the sustainable use of groundwater resources. They also highlight areas where supranational organizations could help fund groundwater deployment programs to improve access to water and area where groundwater resources should be very closely monitored when new WPSs are deployed. Finally, by comparing the MIP to the population density, they also help identify regions where the groundwater resources can be sustainably abstracted to meet the water demand of dense neighbouring populations, where the potential for sustainable abstraction may be lower.

# Methods

**Estimation of the maximum annual pumpable volume.** At a given location, we define the maximum annual pumpable volume, normalized by unit of surface, as:

$$V_{max} = \alpha_R \cdot R + \alpha_S \cdot S \tag{1}$$

where $\alpha_R$ and $\alpha_S$ are respectively the percentage of the groundwater recharge that we accept to pump and the percentage of the groundwater storage that we accept to pump per year.

To estimate the annual volume that can still be pumped, data on the current groundwater withdrawal are needed. Huang et al.[42] estimate the water withdrawal worldwide with a high resolution thanks to public datasets from different sectors for the last 40 years with a time step of one month. Huang et al.[42] provide data on water withdrawal for domestic use, mining, generating electricity, manufacturing, livestock and irrigation. Huang et al.[42] provide 4 different estimations of the water withdrawal for irrigation. To work conservatively, we take for each pixel the maximum value of the 4 estimates. We also suppose here that all of the water withdrawal comes from the groundwater resources which is a very conservative hypothesis[25] because water is usually also withdrawn from surface water sources. However, the degree of conservativeness of this assumption varies depending on the location.

We work with data from 2010 (the most recent available year) and we sum the water withdrawals from the 12 months of 2010 to have an annual estimation of the water withdrawal and to be able to compare it to the maximum annual pumpable volume. By summing the water withdrawal from every sector, we obtain an estimation of the total water withdrawal $TWW$ at each location of Africa. Finally, we define the maximum annual volume that can still be pumped, normalized by surface unit, as:

$$V'_{max} = \alpha_R \cdot R + \alpha_S \cdot S - TWW \tag{2}$$

**Estimation of the maximum installable power.** We define the maximum installable power (MIP) at a location as the sum of the power of every WPS that can be installed in a 1 km$^2$ area at this location not to overshoot the maximum annual pumpable volume. To work conservatively, we consider a field of several pumps of minimum power $P_0$ because $N_{syst}$ pumps of power $P_0$ will pump more than a single pump of power $N_{syst} \cdot P_0$[72,73]. This assumption is more conservative in regions where WPSs are mainly used for irrigation, which requires more powerful WPSs[74]. In all the article, the power of the pumps $P_0$ is taken equal to 100W. Additionally, to be conservative, we also suppose that the WPS is pumping continuously for 365 days at the constant power $P_0$. The MIP is defined as:

$$MIP = N_{syst} \cdot P_0 \tag{3}$$

where $N_{syst}$ is the maximum number of WPSs that can be installed not to overshoot the maximum annual pumpable volume. It is given by:

$$N_{syst} = \frac{V_{max} \cdot S_{area}}{v_p} \tag{4}$$

where $V_{max}$ is the maximum annual pumpable volume, $S_{area}$ is the surface of the considered area, equal to 1 km$^2$ in this article, and $v_p$ is the annual pumped volume by a single WPS of power $P_0$. To estimate the maximum remaining installable power (and thus account for the current water withdrawal), $V_{max}$ should be replaced by $V'_{max}$ (see Equation (2)). Equation (4) implies that we neglect the possible hydrogeological interaction between neighbouring pumping systems, which is conservative because $N_{syst}$ systems which interact pump less than if they do not[75]. This assumption tends to be more conservative in denser areas, like in an urban area where there may be many WPSs close to each other's. $v_p$ is determined from the profile of the pumped flow rate $Q$ during the year:

$$v_p = \int_{1\,year} Q(t)dt \tag{5}$$

For a WPS, the Bernoulli theorem gives the following relation between the pumped flow rate $Q$, the power $P_0$ and the total dynamic head $TDH$ :

$$Q(t) = \frac{P_0 \cdot \eta_{pu}}{\rho \cdot g \cdot TDH(t)} \tag{6}$$

where $\eta_{pu}$ is the pump efficiency, $\rho$ the water density (equal to 1000 kg/m$^3$) and $g$ the gravitational acceleration (equal to 9.81 m/s$^2$). The total dynamic head $TDH$ is given by[35]:

$$TDH(t) = H_b(t) + H_p(t) \tag{7}$$

where $H_b$ is the water depth in the borehole and $H_p$ is the additional head due to pressure losses in the pipe. $H_p$ is given by[76]:

$$H_p(t) = H_{p,ma}(t) + H_{p,mi}(t) \tag{8}$$

where $H_{p,ma}$ corresponds to losses that occur along the length of the pipe (often referred to as "major losses") and $H_{p,mi}$ corresponds to losses at junctions such as curvatures and elbows (often referred to as "minor losses"). $H_{p,ma}$ and $H_{p,mi}$ are given by[40,47,76]:

$$H_{p,ma}(t) = \gamma \cdot L_p \cdot Q^2(t) \tag{9}$$

$$H_{p,mi}(t) = K \cdot Q^2(t) \tag{10}$$

where $L_p$ is the pipe length, $\gamma$ is the linear pipe losses coefficient (see reference [40]) and $K$ is the junction losses coefficient. The water depth in the borehole $H_b$ is given by[77]:

$$H_b(t) = H_{b,s} + H_{b,d}(t) \tag{11}$$

where $H_{b,s}$ is the static water depth and $H_{b,d}$ is the drawdown. The drawdown is composed of two parts:

$$H_{b,d}(t) = H_{b,d}^b(t) + H_{b,d}^a(t) \tag{12}$$

where $H_{b,d}^b$ is the head loss due to borehole losses and $H_{b,d}^a$ is the head loss due to aquifer losses. The head loss due to borehole losses $H_{b,d}^b$ is given by[48]:

$$H_{b,d}^b(t) = \beta \cdot Q(t)^2 \tag{13}$$

where $\beta$ is the borehole losses coefficient. By integrating Equations (7), (8), (9), (10), (11), (12) and (13) into Equation (6), we obtain the pumped flow rate profile $Q$ by solving:

$$\forall t, \quad \left(\beta + \gamma \cdot L_p + K\right) \cdot Q(t)^3 + H_{b,s} \cdot Q(t) + H_{b,d}^a(t) \cdot Q(t) - \frac{P_o \cdot \eta_{pu}}{\rho \cdot g} = 0 \tag{14}$$

The expression of $H_{b,d}^a$ depends on whether the system is extracting water from a confined or an unconfined aquifer. Indeed, by considering that the flow rate varies (because the drawdown varies), $H_{b,d}^a$ is given by the following expressions depending on the type of aquifer[73,75]:

$$H_{b,d,conf}^a(t) = \frac{1}{4\pi T} \int_0^t Q(\tau) \cdot \frac{e^{-\frac{S_y \cdot r_b^2}{4T(t-\tau)}}}{t-\tau} d\tau \tag{15}$$

$$H_{b,d,unconf}^a(t) = H_{st} \left(1 - \sqrt{1 - \frac{1}{2\pi T \cdot H_{st}} \int_0^t Q(\tau) \cdot \frac{e^{-\frac{S_y \cdot r_b^2}{4T(t-\tau)}}}{t-\tau} d\tau}\right) \tag{16}$$

where Equation (15) estimates the head loss due to aquifer losses if the aquifer is confined, and Equation (16) if the aquifer is unconfined. $T$ is the aquifer transmissivity and $S_y$ the storativity. Unfortunately, no mapped data for the aquifer storativity $S_y$ is provided. Based on the literature, $S_y$ is comprised between 0.1 and 0.3 for unconfined aquifers and between $10^{-5}$ and 0.005 for confined aquifers[78–80]. To underestimate the $TDH$, and thus to be conservative, we choose the maximum value of $S_y$ in its respective ranges (i.e., 0.3 for an unconfined aquifer, and 0.005 for a confined one). Moreover, to our best knowledge, there is no data on whether major aquifers are confined or unconfined for any location across Africa. Therefore, to ensure the conservativeness of our results, we estimate both the annual pumped volume by a single WPS $v_p$ by considering the aquifer confined and unconfined and we finally choose the maximum volume. By integrating Equation (15) or (16) into Equation (14), we see that Equation (14) is a nonlinear equation. When considering the aquifer confined, Equation (14) is a polynomial equation and we take the only physically feasible solution of the equation. When considering the aquifer unconfined, Equation (14) is more complex and we use the Newton Raphson method. The method is initialized at each time step with a chosen value $Q^0$. To allow the convergence of Equation (14), we choose $Q^0$ as the solution of Equation (6) when considering $H_{b,s}$ and $H_{b,d}^a$ equal to 0. This yields $Q^0$ = 0.0052 m$^3$/s.

Once $Q(t)$ is determined, we compute $H_{b,d,conf/unconf}^a(t)$ thanks to Equation (15) or (16). If the water depth in the borehole $H_b$ is found to be deeper than the pump depth $H_{pu}$, then we set $Q(t)$ to 0 (i.e., the pump stops) for a period $\Delta t_{shut}$[35] (see Supplementary Figure 3). After this period $\Delta t_{shut}$, the pump attempts to restart[35].

To implement Equation (15) and Equation (16), we first considered that the flow rate varies at each one-minute time-step To reduce calculation-time, we investigated the possibility of considering a two-minute time-step instead of a one-minute time-step. Based on results of our model for 200 randomly chosen locations across Africa, this approximation leads to an overestimation of the pumped volume $v_p$ for all locations and an average overestimation of 1% with a maximum of 6% (which thus maintains the conservativeness of our model), while dividing the computing time by 4.2. For instance, the computing time to obtain the annual pumped volume by a single WPS in a confined aquifer $v_{p,conf}$ is 14 days with a two-minute time-step while it is of 59 days with a one-minute time-step. Note that the computing times are obtained with the following computer server: Intel Xeon, CPU E5-2643 0, 3.40GHz, 16 cores. Consequently, the calculations for the whole Africa were carried out with a two-minute time step. The obtained annual pumped volume of a single WPS in a confined aquifer $v_{p,conf}$, and the annual pumped volume of a single WPS in an unconfined aquifer $v_{p,unconf}$ are shown in Supplemental note 2.

**Conservative assumptions and choice of the design parameters.** No exact values of the saturated thickness $H_{st}$, the transmissivity $T$, the static water level $H_{b,s}$ and the groundwater storage $S$ are provided for each location but only ranges of variation. For example, for -15.8° (lat) & 21.9° (lon), the saturated thickness is comprised between 25 and 100 m. To ensure the conservativity of our results, we want to overestimate the annual volume pumped by the WPS $v_p$. Consequently, we want to underestimate the drawdown $H_{b,d}$ (see Figure 1) and the losses (see 'Estimation of the maximum installable power' in the Methods Section). To minimize the drawdown $H_{b,d}$, we choose the minimum value of the static water level $H_{b,s}$ and the maximum values of the transmissivity $T$ within their respective ranges. To minimize the number of stops from the pump, we choose the maximum value of the saturated thickness $H_{st}$ within its respective range. Regarding groundwater storage $S$, since the conservativity of groundwater storage is set by the percentage of groundwater storage that we accept to withdraw each year $\alpha_S$, we choose at each pixel the mean of the range for the groundwater storage $S$.

Regarding the design parameters, to ensure the maximum efficiency of the pump $\eta_{pu}$ and thus the highest pumped volume $v_p$, we choose $\eta_{pu}$ as the highest efficiency of all the feasible efficiencies of the different types of pumps (photovoltaic, diesel…). We consider a realistic minimum shutdown time of the pump before attempting to restart $\Delta t_{shut}$ to limit time without pumping. We suppose a maximum realistic value for the borehole radius to minimize the drawdown[73] and to allow for a maximum realistic value for the pipe diameter to limit the pipe losses[76]. To limit the pipe losses, we also consider a minimum realistic value for the pipe roughness, and we only consider one elbow[40]. The values of the design parameters chosen in this article are all summarized in Table 2.

Finally, we observe in Table 1 that the location-dependent data have varying spatial resolutions. In this article, we use a spatial resolution of 0.2°. We apply this resolution of 0.2° to all datasets by nearest interpolation. Due to the lack of available information, the input groundwater data provided in Table 1 are considered to remain constant over time[40]. The values chosen for the location-dependent data are shown in Figure 2.

# Data availability

The data used in this study are publicly available at the following links: https://www2.bgs.ac.uk/groundwater/international/africanGroundwater/mapsDownload.html, https://www2.bgs.ac.uk/nationalgeosciencedatacentre/citedData/catalogue/45d2b71c-d413-44d4-8b4b-6190527912ff.html, https://sedac.ciesin.columbia.edu/data/set/gpw-v4-population-density-rev11, and https://doi.org/10.5281/zenodo.897933.

# Code availability

The code can be made available upon reasonable request from simon.meunier@centralesupelec.fr.

# References


1. Wada, Y., & Bierkens, M. F. P. Sustainability of global water use: past reconstruction and future projections. *Environmental Research Letters* 9, 104003 (2014).
2. United Nations, Department of Economic and Social Affairs. World population prospects 2019, Highlights (2019).
3. Nieuwoudt, W. L., Backeberg, G. R., & Du Plessis, H. M. The value of water in the South African economy: Some implications. *Agrekon* 43, 162-183 (2004).
4. Altchenko, Y., & Villholth, K. G. Mapping irrigation potential from renewable groundwater in Africa – a quantitative hydrological approach. *Hydrology and Earth System Sciences* 19, 1055-1067 (2015).
5. Siebert, S., et al. Groundwater use for irrigation – a global inventory. *Hydrology and Earth System Sciences* 14, 1863-1880 (2010).
6. MacDonald, A. M., Bonsor, H. C., Dochartaigh, B. E. O., & Taylor, R. G. Quantitative maps of groundwater resources in Africa. *Environmental Research Letters* 7, 024009 (2012).

7. Schmoll, O., Howard, G., Chilton, J., & Chorus, I. Protecting groundwater for health. Managing the quality of drinking-water sources. World Health Organization (IWA Publishing, 2006).

8. MacDonald, A. M., et al. Groundwater and resilience to drought in the Ethiopian highlands. *Environmental Research Letters* 14, 095003 (2019).

9. Taylor, R. G., et al. Ground water and climate change. *Nature climate change* 3, 322-329 (2013).

10. Calow, R. C., MacDonald, A. M., Nicol, A. L., & Robins, N. S. Ground water security and drought in Africa: linking availability, access, and demand. *Groundwater* 48, 246-256 (2010).

11. MacAllister, D. J., MacDonald, A. M., Kebede, S., Godfrey, S., & Calow, R. Comparative performance of rural water supplies during drought. *Nature communications* 11, 1099 (2020).

12. Konikow, L. F., & Kendy, E. Groundwater depletion: A global problem. *Hydrogeology Journal* 13, 317-320 (2005).

13. Perrone, D., & Jasechko, S. Deeper well drilling an unsustainable stopgap to groundwater depletion. *Nature Sustainability* 2, 773-782 (2019).

14. Smith, R., Knight, R., & Fendorf, S. Overpumping leads to California groundwater arsenic threat. *Nature communications* 9, 2089 (2018).

15. Olen, S. M. Water bankruptcy in Iran. *Nature sustainability* 4, 924-924 (2021).

16. Abd-Elhamid, H. F., & Javadi, A. A. Impact of sea level rise and over-pumping on seawater intrusion in coastal aquifers. *Journal of Water and Climate Change* 2, 19-28 (2011).

17. Tay, C., et al. Sea-level rise from land subsidence in major coastal cities. *Nature Sustainability* 5, 1049-1057 (2022).

18. United Nations. Goal 12: Ensure sustainable consumption and production patterns: https://sdgs.un.org/goals/goal12 (2023).

19. Konikow, L. F. Contribution of global groundwater depletion since 1900 to sea-level rise. *Geophysical Research Letters* 38 (2011).

20. Scanlon, B. R., et al. Groundwater depletion and sustainability of irrigation in the US High Plains and Central Valley. *Proceedings of the National Academy of Sciences* 109, 9320-9325 (2012).

21. Rodell, M., Velicogna, I., & Famiglietti, J. S. Satellite-based estimates of groundwater depletion in India. *Nature* 460, 999-1002 (2009).

22. Pokhrel, Y. N., et al. Model estimates of sea-level change due to anthropogenic impacts on terrestrial water storage. *Nature Geoscience* 5, 389-392 (2012).

23. Rost, S., et al. Agricultural green and blue water consumption and its influence on the global water system. *Water Resources Research* 44 (2008).

24. Wada, Y., et al. Global depletion of groundwater resources. *Geophysical research letters* 37 (2010).

25. Gleeson, T., Wada, Y., Bierkens, M. F. P., & van Beek, L. P. H. Water balance of global aquifers revealed by groundwater footprint. *Nature* 488, 197-200 (2012).

26. MacDonald, A. M., et al. Mapping groundwater recharge in Africa from ground observations and implications for water security. *Environmental Research Letters* 16, 034012 (2021).

27. Ford, A., et al. Groundwater: the world's neglected defence against climate change. *British Geological Survey, Water Aid* (2022).

28. Molle, F., López-Gunn, E., & van Steenbergen, F. The local and national politics of groundwater overexploitation. *Water Alternatives* 11 (2018).

29. Faysse, N. et al. Agricultural use of groundwater and management initiatives in the Maghreb: challenges and opportunities for sustainable aquifer exploitation. *AFDB Economic Brief* (2011).

30. Verma, S., Durga, N., & Shah, T. Solar irrigation pumps and India's energy-irrigation nexus. *IWMI*, 2 (2018).

31. Ministry of Jal Shakti, Deptt. of Water Resources, RD & GR, Government of India. MI Census. Minor Irrigation Census. State Wise Reports: https://micensus.gov.in/state-wise-reports?shs_term_node_tid_depth_1=58&shs_term_node_tid_depth=172 (2019).

32. Pakistan Bureau of Statistics. Agriculture Statistics of Pakistan 2010-11: https://www.pbs.gov.pk/publication/agriculture-statistics-pakistan-2010-11 (2011).

33. Hou, X., Wang, B., Hu, W., Yin, L., & Wu, H., SolarNet: a deep learning framework to map solar power plants in China from satellite imagery. Preprint at https://arxiv.org/abs/1912.03685 (2019).

34. Jang, H. S., Bae, K. Y., Park, H. S., & Sung, D. K. Solar power prediction based on satellite images and support vector machine. *IEEE Transactions on Sustainable Energy* 7, 1255-1263 (2016).

35. Campana, P. E., et al. Economic optimization of photovoltaic water pumping systems for irrigation. *Energy Conversion and Management* 95, 32-41 (2015).

36. Meunier, S. Optimal design of photovoltaic water pumping systems for rural communities–a technical, economic and social approach. PhD thesis, *Université Paris Saclay* (2019).

37. Xie, H., Ringler, C., & Mondal, M. A. H. Solar or diesel: a comparison of costs for groundwater-fed irrigation in sub-Saharan Africa under two energy solutions. *Earth's Future* 9, e2020EF001611 (2021).

38. Chandel, S. S., Naik, M. N., & Chandel, R. Review of performance studies of direct coupled photovoltaic water pumping systems and case study. *Renewable and Sustainable Energy Reviews* 76, 163-175 (2017).

39. Meunier, S., et al. Sensitivity analysis of photovoltaic pumping systems for domestic water supply. *IEEE Transactions on Industry Applications* 56, 6734-6743 (2020).

40. Meunier, S., Kitanidis, P. K., Cordier, A., & MacDonald, A. M. Aquifer conditions, not irradiance determine the potential of photovoltaic energy for groundwater pumping across Africa. *Communications Earth & Environment* 4, 52 (2023).

41. Bonsor, H. C., & MacDonald, A. M. An initial estimate of depth to groundwater across Africa. *British Geological Survey* (2011).

42. Huang, Z., et al. Reconstruction of global gridded monthly sectoral water withdrawals for 1971–2010 and analysis of their spatiotemporal patterns. *Hydrology and Earth System Sciences* 22, 2117-2133 (2018).

43. Ahmed, A. A., Moharam, B. A., & Rashad, E. E. Improving energy efficiency and economics of motor-pump-system using electric variable-speed drives for automatic transition of working points. *Computers & Electrical Engineering* 97, 107607 (2022).

44. Ducar, I., & Marinescu, C. Increasing the efficiency of motor-pump systems using a vector controlled drive for PMSM application. *International Symposium on Fundamentals of Electrical Engineering (ISFEE), IEEE, Bucharest, Romania* (2014).

45. Grundfos. Grundfos Product Center: https://product-selection.grundfos.com (2023).

46. Agrieuro. Motopompe d'irrigation thermique AGT GP160 - raccords de 50 mm : https://www.agrieuro.fr/motopompe-dirrigation-thermique-agt-gp160-raccords-de-50-mm-p-30304.html (2023).

47. Meunier, S., et al. A validated model of a photovoltaic water pumping system for off-grid rural communities. *Applied Energy* 241, 580-591 (2019).

48. Bierschenk, W. H. Determining well efficiency by multiple step-drawdown tests. *International Association of Scientific Hydrology* (1963).

49. Båverman, G., & Tavoosi, E. Evaluation of a solar powered water pumping system in Mutomo, Kenya: Comparison between a submersible induction motor and a PMSM system. MSc thesis, *Uppsala Universiteit* (2019).

50. Smith, C. C. Rural boreholes and wells in Africa - economics of construction in hard rock terrain. *Journal American Water Works* Association 95, 100-111 (2003).

51. Caton, P. Design of rural photovoltaic water pumping systems and the potential of manual array tracking for a West-African village. *Solar Energy* 103, 288-302 (2014).

52. Barrowman, J. S. The practical calculation of the aerodynamic characteristics of slender finned vehicles. MSc Thesis, *The Catholic University of America* (1967).

53. Damkjaer, S., & Taylor, R. The measurement of water scarcity: Defining a meaningful indicator. *Ambio* 46, 513-531 (2017).

54. Ozano, K., et al. Groundwater: Making the Invisible Visible: FCDO Briefing Pack on Water Governance, Finance and Climate Change. *Institute of Development Studies* (2022).

55. Davis & Shirtliff. Afridev: https://www.davisandshirtliff.com/water-pumps/product/afridev (2023).

56. Water Point Data Exchange. WPdx: https://www.waterpointdata.org/ (2020).

57. Bianchi, M., Palamakumbura, R. N., MacDonald, A. M., & MacDonald, D. M. J. Assessing regional variation in yield from weathered basement aquifers in West Africa and modelling their future groundwater development and sustainability. *Hydrogeology Journal* 31, 257-274 (2023).

58. Tuinhof, A., Foster, S., van Steenbergen, F., Talbi, A., & Wishart, M. Appropriate groundwater management policy for sub-Saharan Africa: In face of demographic pressure and climatic variability. *World Bank* (2011).

59. MacDonald, A. M., & Davies, J. A brief review of groundwater for rural water supply in sub-Saharan Africa. *British Geological Survey* (2000).

60. Gaye, C. B., & Tindimugaya, C. Challenges and opportunities for sustainable groundwater management in Africa. *Hydrogeology Journal* 27, 1099-1110 (2019).

61. Hasell, J., Roser, M., Ortiz-Ospina, E. & Arriagada, P. Poverty. *Our World in Data* https://ourworldindata.org/poverty (2022).

62. Banque mondiale. Niger : la Banque mondiale finance la lutte contre le stress hydrique et l'insécurité alimentaire. https://www.banquemondiale.org/fr/news/press-release/2021/09/30/world-bank-invests-to-combat-water-scarcity-and-food-insecurity-in-niger (2021).

63. African Development Bank (AfDB). Somalie - Projet d'alimentation en eau et d'assainissement des villes de Kismayo et Baidoa - Financement - Rapport d'évaluation : https://www.afdb.org/fr/documents/somalie-projet-dalimentation-en-eau-et-dassainissement-des-villes-de-kismayo-et-baidoa-financement-rapport-devaluation (2021).

64. Umar, R., Ahmed, I., & Alam, F. Mapping groundwater vulnerable zones using modified DRASTIC approach of an alluvial aquifer in parts of Central Ganga Plain, Western Uttar Pradesh. *Journal of the Geological Society of India* 73, 193-201 (2009).
65. Davies, J., et al. Identifying transboundary aquifers in need of international resource management in the Southern African Development Community region. *Hydrogeology Journal* 21, 321-330 (2013).
66. Oiro, S., Comte, J. C., Soulsby, C., MacDonald, A. M., & Mwakamba, C. Depletion of groundwater resources under rapid urbanisation in Africa: recent and future trends in the Nairobi Aquifer System, Kenya. *Hydrogeology Journal* 28, 2635-2656 (2020).
67. Center for International Earth Science Information Network, Columbia University. Gridded population of the world, version 4: population density, revision 11 https://doi.org/10.7927/H49C6VHW (2018).
68. Food and Agriculture Organization of the United Nations (FAO). AQUASTAT: https://www.fao.org/land-water/databases-and-software/aquastat/en/ (2020).
69. Silliman, S. E., Boukari, M., Lougbegnon, L., Azonsi, F. Overview of a multifaceted research program in Bénin, West Africa: An International Year of Planet Earth groundwater project in *Sustaining groundwater resources: A critical element in the global water crisis* (Springer, 2011).
70. McLoughlin, P. F. M. Libya's great manmade river project: prospects and problems. *Natural resources forum* 15, 220-227 (1991).
71. United Nations Economic Commission for Europe (UNECE). Policy Brief: Improving sustainable development in the North Western Sahara Aquifer System through a transboundary nexus approach: https://unece.org/environment-policy/publications/policy-brief-improving-sustainable-development-north-western-sahara (2020).
72. Muskat, M. The flow of homogeneous fluids through porous media (McGraw-Hill, 1937).
73. Bear, J. Hydraulics of groundwater (McGraw-Hill, 1979).
74. Wazed, S. M, Hughes, B. R., O'Connor, D., & Calautit, J. K. A review of sustainable solar irrigation systems for Sub-Saharan Africa. *Renewable and Sustainable Energy Reviews* 81, 1206-1225 (2018).
75. Kasenow, M. Applied ground-water hydrology and well hydraulics (Water Resources Publication, 2001).
76. Munson, B. R., Young,D. F., & Okiishi, T. H. Fundamentals of Fluid Mechanics (Wiley, 2005).
77. Vezin, T., et al. Borehole water level model for photovoltaic water pumping systems. *Applied Energy* 258, 114080 (2020).
78. De Graaf, I. E. M., et al. A global-scale two-layer transient groundwater model: Development and application to groundwater depletion. *Advances in Water Resources* 102, 53-67 (2017).
79. Hajhouji, Y. Modélisation hydrologique du bassin versant de l'oued Rheraya et sa contribution à la recharge de la nappe du Haouz (bassin du Tensift, Maroc). PhD thesis, *Université Paul Sabatier-Toulouse III* (2018).
80. Freeze, R. A., & Cherry, J. A. Groundwater (Prentice-Hall, 1979).



## Acknowledgments

The authors thank C. Masternak for her advice and comments.


## Author contributions

G.Z. conceived the original idea, developed the model, curated data, developed the code and wrote the manuscript draft. S.M., D.J.M, P.K.K and A.M.M conceived the original idea and developed the model. All authors developed the analysis and conclusions and reviewed the manuscript.

## Competing interests

The authors declare no competing interests.